03,16

Magneto-Stark effect influence on intensity of exciton-light coupling for excitonic states with large wave vector

© D.K. Loginov[1], A.V. Donets[2]

[1] SOLAB Spin-optic laboratory, Saint-Petersburg state university, St. Petersburg, Russia
[2] St. Petersburg State University, St. Petersburg, Russia

E-mail: loginov999@gmail.com

Received October 27, 2023
Revised December 7, 2023
Accepted December 7, 2023

The modification in exciton-light coupling due to the magneto-Stark effect is considered for excitonic states with a wave vector which is an order of magnitude greater than the wave vector of light. It is shown that the magnetic field affects on the relative motion of an electron and a hole in a moving exciton as an effective electric field in a potential well with an asymmetric parabolic profile. The asymmetry of this profile at large wave vectors leads to a nonmonotonic dependence of the strentgh of exciton-light coupling on the magnetic field.

Keywords: exciton, magnetic field, Magneto-Stark effect, exciton-light coupling.

DOI: 10.61011/PSS.2024.01.57850.242

1. Introduction

Though the magneto-Stark effect (MSE) was for the first time studied in the second half of the past century [1–3], investigation of this phenomenon is still essential for the present-day research community [4–12]. According to these and other studies, the effect of a magnetic field on a moving exciton may be represented as an effective electric field whose strength is proportional to the product of the exciton motion wave vector and magnetic field strength. Such effective field changes the exciton dipole moment and may be detected in optical spectra by exciton-light coupling variation. It should be noted that all known previously published experimental and theoretical studies of MSE addressed this phenomena either in bulk crystals [4–9] or in two-dimensional systems such as double quantum wells or stacking faults [10–12]. Exciton states observed in such structures are characterized by the exciton wave vector whose value is equal or close to the light wave vector in semiconductors. This circumstance prevents from investigating MSE for excitons with large wave vector.

At the same time, exciton states with wave vectors exceeding the light wave vector by one order of magnitude are observed in optical experiments in so-called wide quantum wells (QW) [13–15]. Wells whose thickness exceeds the exciton Bohr radius by an order of magnitude are referred to as wide wells. Earlier, size exciton motion as a whole [16–28] and the influence of external fields on states with large wave vector were investigated in such QW, see, for example, [29–37].

In particular, it was shown in [29,30] that uniaxial stress along the twofold and fourfold axes may lead to the variation of exciton masses and appearance of the linear in wave vector terms, in the exciton Hamiltonian. According to papers [31–33], electric field in wide QW results in variation of exciton-light coupling and an effect of phase inversion of the spectral oscillations in the reflection spectrum. When investigating exciton optical spectra of wide QW in magnetic field in the Voight geometry, the effects of magneto-induced variation of the exciton mass were detected [34,35]. In the Faraday geometry, magnetic field results in the effect of dependence of the Zeeman splitting of exciton states on the value of the exciton wave vector [36,37].

This study is devoted to theoretical investigation of the MSE effect on exciton-light interaction for exciton states with large wave vector that are usually observed in the optical spectra of wide QW. Such large wave vectors will be referred hereinafter implying that applicable exciton states may be investigated in such wells. Whilst QW themselves and the related features of size quantization are not directly addressed herein. They are indirectly implied, because the addressed exciton states are characterized by large wave vectors.

The remaining part of paper is arranged as follows. The second section describes the exciton Hamiltonian in a magnetic field. The third section reviews the effect of the effective electric field occurring at MSE on the exciton states. The fourth section describes the exciton-light interaction variation due to MSE. The last section is devoted to conclusions.

2. Exciton Hamiltonian moving in the transverse magnetic field

Let's consider an exciton in GaAs crystal moving along the z axis whose direction coincides with the crystallo-

graphic axis [001]. In addition, for the exciton wave vector value and components, $K = K_z$, $K_x = K_y = 0$ are met. The magnetic field vector **B** is directed along the x axis, i. e. $B = B_x$, $B_y = B_z = 0$. The x, y and z axes are directed along the fourfold axes [100], [010] and [010], respectively.

The exciton states observed in the optical experiment in GaAs type materials are formed by the states of a twofold degenerate conduction band Γ_6 and a fourfold degenerate valence band Γ_8. The exciton Hamiltonian is formed by Hamiltonians of free electrons and holes (H_c and H_v) in these bands and their Coulomb interaction

$$\hat{H}_X = E_g + \hat{H}_c + \hat{H}_v - \frac{e^2}{\varepsilon_0 r}, \qquad (1)$$

where E_g is the band gap width, e is the electron charge, ε_0 is the background dielectric permittivity of the crystal, $r = |\mathbf{r}_e - \mathbf{r}_h|$ is the electron-hole distance ($\mathbf{r}_e$ and $\mathbf{r}_h$ are electron and hole radius vectors, respectively).

This Hamiltonian may be expressed through the exciton motion wave vector, K, relative motion moment operators of electrons and holes in the exciton, $\hat{p}_\alpha = -i\hbar\partial/\partial\alpha$, and magnetic field potential vector $\hat{A}_\alpha$ [10,12]. Here, $\alpha = x, y, z$ are the relative motion coordinates of the electron and hole: $x = x_h - x_e$, $y = y_h - y_e$ and $z = z_h - z_e$, where x_h, y_h, z_h and x_e, y_e, z_e are the hole and electron coordinates, respectively. The exciton motion wave vector may be treated as just a number. The potential vector components in the Landau gauge are written as: $(e/c)A_z = (e/c)B \cdot y$ and $A_x = A_y = 0$. It should be noted that the effect discussed below is essentially manifested for the states characterized by high wave vector $K \gg 1/a_B$, where a_B is the exciton Bohr radius. As shown in [38], mixture of heavy-hole and light-hole excitons may be neglected for such wave vectors. In this approximation, energy-wave vector relation for heavy-hole and light-hole excitons is parabolic as for non-degenerate exciton bands. Considering the above, Hamiltonian (1) may be written as

$$\hat{H}_{h(l)} = E_g + \frac{\hbar^2 K^2}{2M_{h(l)}} + \frac{\hat{p}^2}{2\mu} - \frac{e^2}{\varepsilon_0 r} + \left(\frac{e}{c}\right)\frac{\hbar K}{M_{h(l)}} By + \left(\frac{e}{c}\right)^2 \frac{m_e^3 + m_h^3}{2M^2 m_e m_h} B^2 y^2. \qquad (2)$$

Here, the second term is the kinetic energy of a moving exciton that is a constant scalar quantity for the certain wave vector K. $M_{h(l)} = m_e + m_{hh(lh)}$ is the mass of hheavy-hole exciton (index h) and light-hole exciton (index l), where m_e is the effective mass of an electron and $m_{hh(lh)}$ is the mass of heavy-hole (hh) or light-hole (lh). It should be noted that to describe the exciton motion as a whole in an approximation of large wave vectors ($K \gg 1/a_B$, where a_B is the exciton Bohr radius), the mass of heavy- and light-holes are assumed equal to $m_{hh(lh)} = m_0/(\gamma_1 \pm 2\gamma_2)$, where γ_1 and γ_2 are the Luttinger parameters and m_0 is the mass of a free electron, see [38]. The third term describes the kinetic energy of the relative motion of and electron and hole in an exciton. This used a notation for the reduced mass $\mu = m_e m_h/(m_e + m_h)$, where $m_h = m_0/\gamma_1$ is the mass of a hole that has the same value for heavy-hole and light-hole excitons in such approximation [38]. A notation for the squared relative motion momentum operator is also introduced: $\hat{p}^2 = \hat{p}_x^2 + \hat{p}_y^2 + \hat{p}_z^2$. The fifth term in expression (2) contains both the exciton motion wave vector and a relative motion coordinate of an electron and hole. The last term in expression (2) describes the diamagnetic exciton shift, where an expression for the mass of exciton $M = m_e + m_h$ is used.

Expression (2) shall also contain a term describing the Zeeman splitting in a magnetic field: $\mu_B(g_e\sigma_x + g_h J_x)B$. here, σ_x is the Pauli matrix and J_x is the angular moment matrix of a hole, g_e and g_h are g-factors of an electron and hole, respectively; μ_B is the Bohr magneton. The analysis shows that in the magnetic fields for GaAs addressed below, the energy variation described by this operator is much lower than the energy variations described by the remaining terms in expression (2), therefore, the Zeeman splitting is not discussed below.

In such scenario, the effects of mixture of heavy-hole and light-hole exciton states may be neglected, because their contributions to the energy are low compared with the rest contributions addressed herein. This allows the heavy-hole and light-hole exciton states to be considered independently from each other within the approximations used herein.

To further simplify the problem, it should be noted that, in QW on the basis of GaAs/AlGaAs compounds, contribution of light-hole excitons to spectra is significant only near the main optical transition of a light-hole exciton for which the wave vector is $K = q$ (q is the wave vector of light). At the same time, the exciton-light coupling variations addressed herein are significant only at large exciton wave vectors such as $K \gg q$. Therefore, below we shall restrict ourselves only to the case of heavy-hole exciton states that are most vividly revealed in optical experiments.

3. Magneto-Stark effect for large exciton wave vectors

In order to find the energy and wave functions of the relative motion of an electron and hole in an exciton, Hamiltonian eigenproblem (2) shall be solved. Since the analytical solution of such problem has not been found yet, we will solve it numerically. For this purpose, it is convenient to pass from a Cartesian to cylindrical coordinate system according to the expressions, see, for example, [13]:

$$\rho = \sqrt{x^2 + z^2}, \quad y = y, \quad \phi = \arctan g(x/z). \qquad (3)$$

If the first two terms in (2) are omitted, which may be assumed as constant numbers at fixed K, then after pass to cylindrical coordinates and considering the above

approximations, this Hamiltonian is written as

$$\hat{H}_h = -\frac{\hbar^2}{2\mu}\left(\frac{\partial^2}{\partial\rho^2} + \frac{1}{\rho}\frac{\partial}{\partial\rho} + \frac{\partial^2}{\partial z^2}\right) - \frac{e^2}{\varepsilon_0\sqrt{\rho^2+y^2}} - eF_{KB}y + DB^2y^2. \quad (4)$$

The notations

$$F_{KB} = \hbar KB/(M_h c)$$

and

$$D = (e/c)^2(m_e^3 + m_h^3)/(2M^2 m_e m_h)$$

are introduced here. This expression does not contain derivatives with respect to ϕ, because only the symmetric ground state of the exciton is considered which does not depend on this variable.

It should be noted that the third term in expression (4) may be formally represented as a contribution to energy from the effective electric field depending on the product of the wave vector and magnetic field. Exciton state variation under the action of such effective field was addressed earlier in literature as the magneto-Stark effect [1–9]. The last term in (4) describes the diamagnetic exciton shift which makes positive contribution to the exciton energy. Of this term may be assumed as a confiment along the y coordinate of electron and hole motion in the exciton, besides the Coulomb summand, also by the parabolic potential. The slope of such potencial well depends on the squared magnetic field. This parabolic potential prevents exciton ionization by the effective electric field F_{KB}, which tends to spread the electron and hole along the y axis.

Thus, the relative motion energy of the electron and hole in a sufficiently strong magnetic field may be regarded as the magneto-Stark effect in a parabolic well. Full potential considering MSE is derived from three last terms in expression (4) and is written as

$$U(K,B) = -\frac{e^2}{\varepsilon_0\sqrt{y^2+\rho^2}} - eF_{KB}y + DB^2y^2. \quad (5)$$

As can be seen, (5) depends on the applied field and on the exciton motion wave vector.

Numeric solution of the problem of finding the Hamiltonian wave functions (4) shall be found using the representations of derivatives with difference schemes on a finite discrete coordinate grid [39]. Since this operator includes second derivatives with respect to two variables, solution of the problem of finding the operator eigenfunctions is limited to the diagonalization of a seven-diogonal matrix.

Wave function calculation data is shown in Figure 1, *a, b, c*. The calculations used the following material constants of bulk GaAs: Luttinger parameters $\gamma_1 = 6.8$ and $\gamma_2 = 2.2$, effective electron mass $m_e = 0.066m_0$ [40]; background dielectric permittivity $\varepsilon_0 = 12.56$ [41]. Comparing Figure 1, *a, b* with Figure 1, *c*, it could be seen that the magnetic field for the moving exciton results in the shift of the wave function peak along the y axis relative to the origin of coordinates. This shift is associated with the action of effective electric field F_{KB}. As shown in Figure 1, *d*, the effective field results in asymmetric distortion of potential (5) and, in displacement of the wave function peak from point $\rho = 0$, $y = 0$ along the y axis.

4. Influence of the magneto-Stark effect on longitudinal and transverse exciton splitting

Intensity of the exciton-light coupling may be expressed through the degree of longitudinal-transverse splitting [9,13,14]. From knowing the relative motion functions of the electron and hole in the exciton, it is possible to calculate exciton longitudinal-transverse splitting using expression [13]:

$$\hbar\omega_{LT} = \left(\frac{2eP_1}{E_g}\right)^2 \frac{\pi}{\varepsilon_0}|\psi(0)|^2. \quad (6)$$

Here, $\psi(0)$ is the relative motion wave function with $r = 0$; constant $P_1 = \hbar p_{cv}/m_0$, where p_{cv} is the interband matrix element of the electron momentum. For GaAs, $P_1 = 10.3 \cdot 10^{-5}\,\text{meV}\cdot\text{cm}$ [42]. As shown in Figure 1, $\psi(0)$ shall depend on the wave vector of the applied magnetic field. Therefore, the longitudinal-transverse splitting will also depend on K and B.

Calculation of the longitudinal-transverse exciton splitting considering MSE is shown in Figure 2. As can be seen, an increase in the field for the exciton at rest ($K = 0$) results in gradual increasing of $\hbar\omega_{LT}$. This is associated with the fact that with magnetic field increasing the effective potential confining the electron-hole pair motion in the exciton increases and the wave function localization region becomes narrow due to the diamagnetic effect (Figure 1, *d*). In this case, the probability of finding the electron and hole at the origin of coordinates increases resulting in growth of $\hbar\omega_{LT}$ according to expression (6).

At the same time, with $K \neq 0$, the effective electric field results in an opposite effect: the growth of longitudinal-transverse splitting in the field becomes lower than with $K = 0$. Moreover, with $K = 2.5 \cdot 10^6\,\text{cm}^{-1}$, magnetic field growth up to $B \leq 1.5\,\text{T}$ results in decrease in $\hbar\omega_{LT}$. This is associated with potential profile distortion along the y axis as shown in Figure 1, *d*. In such distorted potential, the relative motion wave function peak moves from the origin of coordinates as shown in Figure 1, *c*. This results in a decrease in $|\psi(0)|^2$ and, as follows from expression (6), in a decrease in the longitudinal-transverse splitting as shown in Figure 2. In magnetic field $B > 1.5\,\text{T}$, diamagnetic contribution to $\hbar\omega_{LT}$ becomes higher than the contribution of the effective electric field, and the longitudinal-transverse splitting starts growing with an increase in B even for $K = 2.5 \cdot 10^6\,\text{cm}^{-1}$.

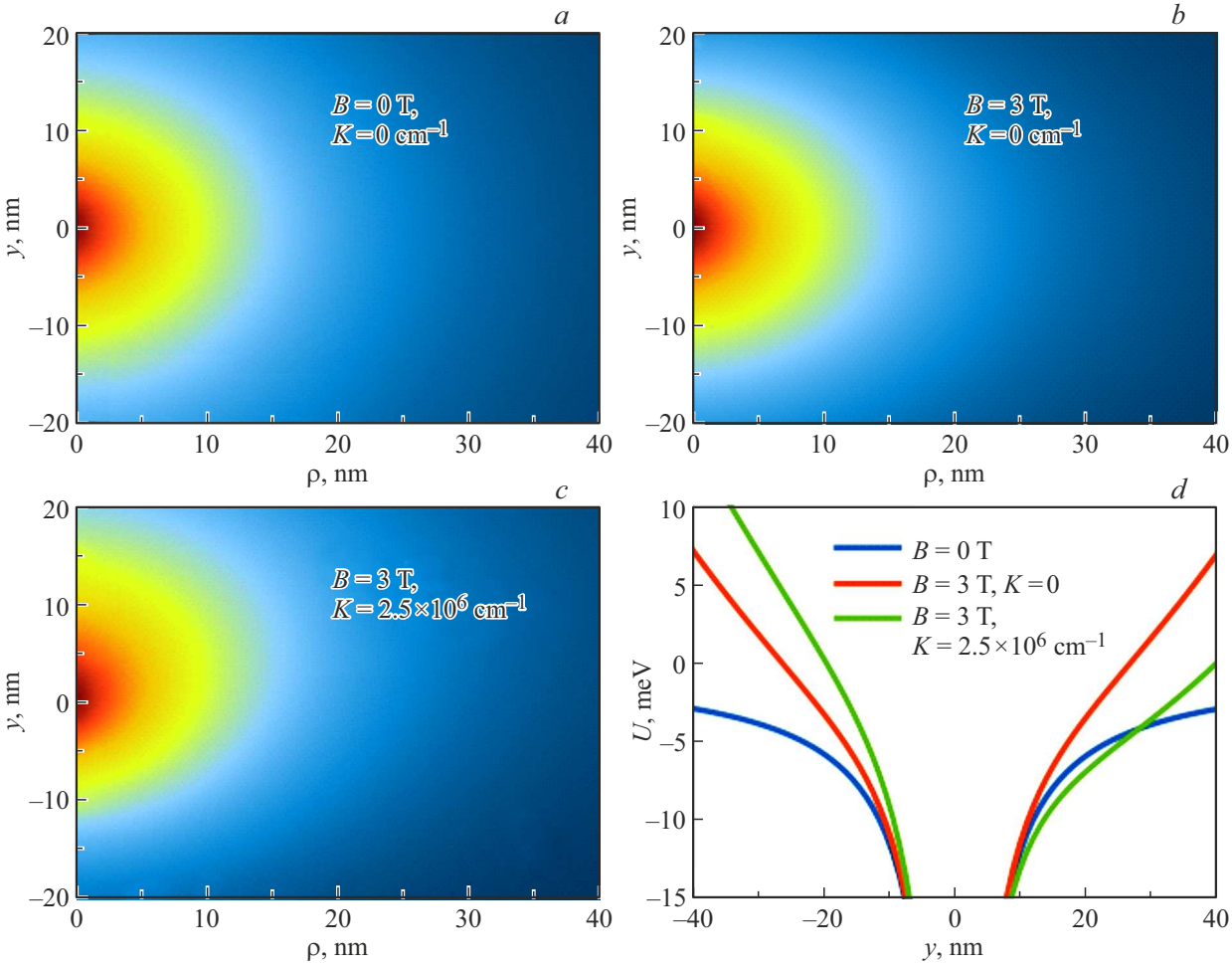

Figure 1. Wave functions of the exciton ground state: *a* — calculated without any field; *b* — in field $B = 3\,\mathrm{T}$ for an exciton at rest and *c* — in field $B = 3\,\mathrm{T}$ for a moving exciton with wave vector $K = 2.5 \cdot 10^6\,\mathrm{cm}^{-1}$; pane (*d*) — potential profile $U(K, B)$ for the relative motion of an electron and hole taken at $\rho = 0$ (see expression (5)).

In relatively small fields, the longitudinal-transverse splitting shall depend on squared magnetic field and wave vector in accordance with the perturbation theory. Therefore, with $B < 0.9\,\mathrm{T}$, positions of points in Figure 2 shall be approximated by expression

$$\hbar\omega_{LT}(K, B) = d(K)B^2 + \hbar\omega_{LT}(0). \qquad (7)$$

Here, $\hbar\omega_{LT}(0)$ is the longitudinal-transverse splitting without magnetic field which, according to expression (6) and when using material constant given above, is equal to 0.0663 meV. Values of $d(K)$ in function of the wave vector are shown in Figure 3. Positions of reference points in this Figure are described by expression

$$d(K) = \delta \cdot K^2 + \gamma_d, \qquad (8)$$

where constant coefficients are as follows

$$\delta = 1.4 \cdot 10^{-15}\,\mathrm{meV} \cdot \mathrm{T}^{-2} \cdot \mathrm{cm}^{-2}$$

and

$$\gamma_d = 0.0037\,\mathrm{meV} \cdot \mathrm{T}^{-2}.$$

The first term in (8) is associated with MSE, which describes a term containing F_{KB} in expressions (4) and (5). The second describes square-law variation of $\hbar\omega_{LT}$ in magnetic field due to the diamagnetic effect.

As shown in Figure 2, in field $B \approx 0.9\,\mathrm{T}$ and for $K \geq 2 \cdot 10^6\,\mathrm{cm}^{-1}$, reference points are poorly described by functions written as (7) and (8). This may be explained by the fact that at such values of the wave vector and magnetic field, the perturbation theory, from which square-law dependence of $\hbar\omega_{LT}$ on F_{KB} is derived, is not applicable. For approximation of point positions in the Figure at $B > 0.9\,\mathrm{T}$, the following more complicated expressions shall be used

$$\hbar\omega_{LT}(K, B) = a(K)B^2 + b(K)|B| + \hbar\omega_{LT}(0). \qquad (9)$$

Here, the term proportional to $|B|$ is attributed to the effect of the diamagnetic shift on the exciton-light coupling. As shown, for example, in [34], with $B > 1\,\mathrm{T}$, terms that are linear in $|B|$ occur in expressions for the diamagnetic shift of exciton energy vs. magnetic field. This results in

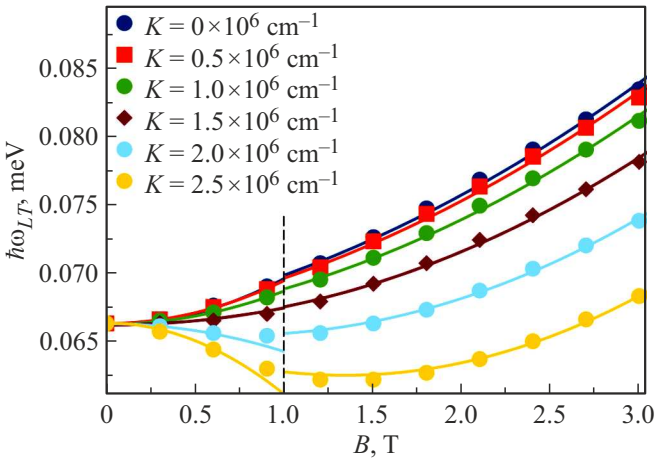

Figure 2. Calculated longitudinal-tranvers exciton splitting in magnetic fields from 0 to 3 T and for exciton wave functions K from 0 to $2.5 \cdot 10^6$ cm^{-1}. Points are calculated values of $\hbar\omega_{LT}$. Solid curves are approximations by expressions (7) and (8) in fields $B \leq 0.9$ T and expressions (9) and (10) with $B > 0.9$ T.

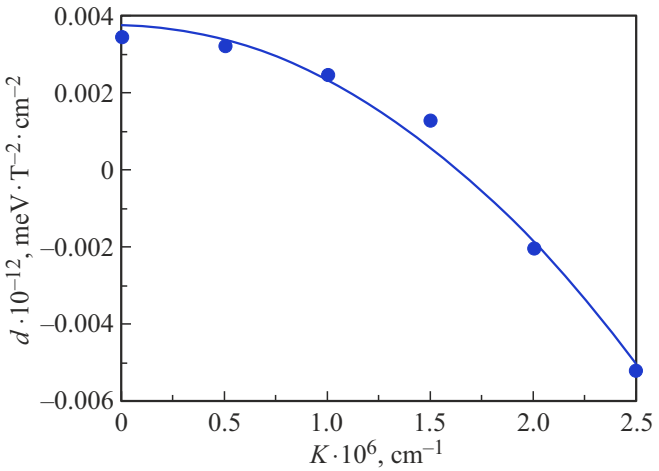

Figure 3. d values in expression (7) with different K. Solid curves are approximations by expression (8).

occurrence of the similar summand in the expression for the longitudinal-tranvers splitting in (9). It should be noted that it is the second term in expression (9) that describes nonmonotonicity of variation of $\hbar\omega_{LT}$ with an increase in B in Figure 2.

Values of a and b in expression (9) are shown in Figure 4. Positions of reference points may be approximated by expressions

$$a(K) = \alpha K^2 + \gamma_a,$$
$$b(K) = \beta K^2 + \gamma_b. \qquad (10)$$

These dependences are shown in Figure 3 as solid curves. Coefficients in expressions (10) have the following values:

$$\alpha = 1.5 \cdot 10^{-16}\,\text{meV} \cdot \text{cm}^2 \cdot \text{T}^{-2},$$
$$\gamma_a = 1.1 \cdot 10^{-3}\,\text{meV} \cdot \text{T}^{-2}$$

and

$$\beta = -1.3 \cdot 10^{-15}\,\text{meV} \cdot \text{cm}^2 \cdot \text{T}^{-1},$$
$$\gamma_b = 2.6 \cdot 10^{-3}\,\text{meV} \cdot \text{T}^{-1}.$$

Like in expression (8), the first summands in the right-hand side are described by F_{KB}-dependent terms in expressions (4) and (5). The second summands in the right-hand side of each of expressions (10) describe the influence of the diamagnetic effect on the exciton-light coupling. Thus, an expression was derived to allow quantitative description of the above effect.

Note that the effect describe above may be observed experimentally only for states with large wave vector $K \gg 1/a_B$ [38]. Such states may be observed in optical spectra of wide QW. To assess how vividly this effect shall be revealed in optical experiments, we calculated the QW reflection spectra based on GaAs/$Al_{0.3}Ga_{0.7}As$. The calculation implied that the structure consists of a 290 nm barrier with a background dielectric permittivity of $\varepsilon_b = 11$, GaAs well layer with thickness $L_{QW} = 210$ nm and semi-infinite barrier layer with permittivity $\varepsilon_b = 11$. Background dielectric permittivities of barriers approximately correspond to that of ternary $Al_{0.3}Ga_{0.7}As$ solution. Reflection spectra calculation used a bulk polariton modes interference model in a semiconductor plate with Pekar's addition boudary condition, see, for example, [15,16,18]. The calculations used the same values of GaAs variables as for the longitudinal-tranvers splitting calculation. Also, the nonradiative exciton attenuation parameter in GaAs layer was assumed equal to $\Gamma = 0.1$ meV. Figure 5 shows the reflection spectra of such QW calculated without a magnetic field and in field $B = 3$ T.

The left-hand half of the figure shows the amplitude-dominating feature of reflection associated with the basic optical transition of a heavy-hole exciton. The right-hand half shows a zoomed in region that contains scattering reflection oscillations that attenuate towards the high energy

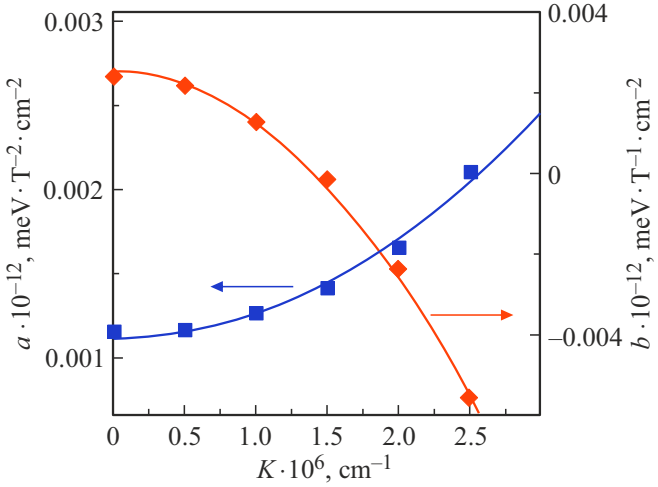

Figure 4. Values of a and b in expression (9) at various K. Solid curves are approximations by expressions (10).

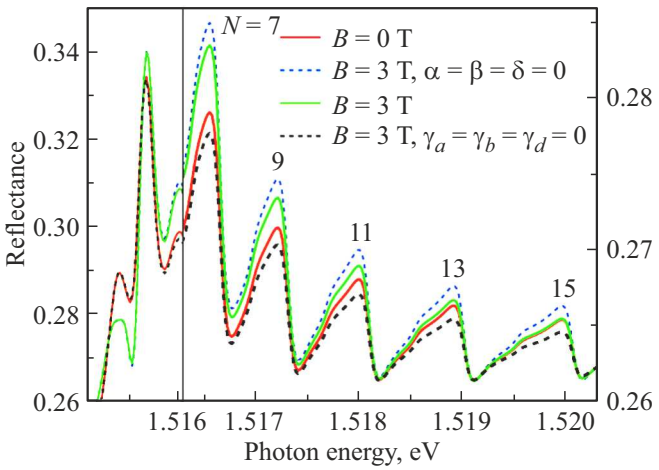

Figure 5. Reflection spectra calculated for a $L_{QW} = 210$ nm $GaAs/Al_{0.3}Ga_{0.7}As$ QW without magnetic field (red solid line) and in field $B = 3$ T (green solid line). The blue dashed curve shows the spectrum in the same magnetic field calculated without considering MSE, but considering the contribution of the diamagnetic effect to the exciton-light coupling. The black dashed curve is the calculated spectrum in magnetic field considering MSE, but without considering the diamagnetic effect. Digits near the reflection oscillations mean the size quantization level number N corresponding to this spectral feature.

region and are associated with the exciton size quantization levels, see [13–15]. An exciton motion size quantization level with number N is assigned to each of such oscillations.. This number is associated with the exciton motion wave vector as a whole by expression: $K = 2\pi N/L_{QW}$. It should be noted that either even or odd numbers of size quantization levels are assigned to each oscillation in the reflection spectra [15]. Moreover, the first several levels fall into the main peak region and are not visible against its background, see, for example, [17,34].

To visualize the effect in question, we have moved the spectra on the energy axis to make sure that positions of amplitude-dominating oscillations coincide in all spectra. In addition, we did not consider the effective exciton mass variation in a magnetic field which also results from MSE and was discussed earlier, for example, in [34,35].

Comparison of the reflection spectra calculated for $B = 0$ and $B = 3$ T shows that the spectral oscillation amplitudes in magnetic field increase compared with the amplitudes of the same oscillations without magnetic field. This difference is maximum for the dominating reflection oscillation associated with the basic optical transition of the exciton. Increase in amplitude in magnetic field is caused by the diamagnetic effect on the light exciton interaction that is described by constants γ_d in expression (8) and by γ_a, γ_b in expression (10). For oscillations associated with the exciton motion size quantization levels, an increase in the oscillation amplitude in magnetic field becomes lower with increasing N, i. e. exciton wave vector. In particular, for an oscillation with $N = 15$, the amplitude in field $B = 3$ T becomes equal to the amplitude of the same oscillation in field $B = 0$. Magneto-induced decrease in amplitude depending on the exciton wave vector is caused by MSE and described by δ in expression (8) and by α, β in expression (10).

To demonstrate the diamagnetic effect and MSE separately, Figure 5 also shows the spectra calculated at $\delta = \alpha = \beta = 0$ and $\gamma_d = \gamma_a = \gamma_b = 0$, respectively. As can be seen, when only the diamagnetic effect ($\delta = \alpha = \beta = 0$) is considered, magnetic field causes an increase in amplitudes of all oscillations in the spectrum approximately by 20% regardless of their wave vector (N). At the same time, when the effect of only MSE ($\gamma_d = \gamma_a = \gamma_b = 0$) on the light-exciton interaction is considered, then only a decrease in the reflection oscillation amplitude occurs in magnetic field with an increase in N. An exception in this case is the amplitude-dominating reflection feature of the optical transition of the exciton for which the wave vector is small. Therefore, the MSE effect on the light-exciton interaction for this reflection oscillation is negligible compared with other oscillations in the spectrum.

As far as we know, experimental exciton spectra of wide QW in magnetic field have not been reviewed before for the dependence of the longitudinal and transverse exciton splitting on the wave vector. To check the findings obtained herein, further experimental investigations are required.

5. Conclusion

The longitudinal-tranvers exciton splitting under the magneto-Stark effect was calculated for large exciton wave vectors. It is shown that, on the one hand, the effective electric field results in a decrease in the exciton-light coupling. The exciton-light coupling strength becomes lower with increasing product of the magnetic field strength and exciton wave vector. On the other hand, the diamagnetic exciton energy shift facilitates an increase in the exciton-light coupling strength. Thanks to the diamagnetic shift, this intensity grows with squared magnetic field and does not depend on the wave vector. As a result of simultaneous effect of the two factors, the exciton-light coupling for states with sufficiently large wave vector should vary non-monotonously with growth of the applied magnetic field.

Funding

The study was supported by grant No .94030557 provided by St. Petersburg State University.

Conflict of interest

The authors declare that they have no conflict of interest.

References

[1] E.F. Gross, B.P.Zakharchenya, O.V. Konstantinov. FTT **3**, 221 (1961). (in Russian).
[2] D.G. Thomas, J.J. Hopfield. Phys. Rev. B **124**, 657 (1961).
[3] L.P. Gorkov, I.E. Dzyaloshinskiy, ZhETF **26**, 449 (1968). (in Russian).
[4] B.S. Monozon, P. Schmelcher. Phys. Rev. B **82**, 205313 (2010).
[5] M. Lafrentz, D. Brunne, B. Kaminski, V.V. Pavlov, A.V. Rodina, R.V. Pisarev, D.R. Yakovlev, A. Bakin, M. Bayer. Phys. Rev. Lett. **110**, 116402 (2013).
[6] M. Lafrentz, D. Brunne, A.V. Rodina, V.V. Pavlov, R.V. Pisarev, D.R. Yakovlev, A. Bakin, M. Bayer. Phys. Rev. B **88**, 235207 (2013).
[7] A. Farenbruch, J. Mund, D. Frohlich, D.R. Yakovlev, M. Bayer, M.A. Semina, M.M. Glazov. Phys. Rev. B **101**, 115201 (2020).
[8] P. Rommel, J. Main, A. Farenbruch, J. Mund, D. Fröhlich, D.R. Yakovlev, M. Bayer, C. Uihlein. Phys. Rev. B **101**, 115202 (2020).
[9] I.Y. Chestnov, S.M. Arakelian, A.V. Kavokin. New J. Phys. **23**, 023024 (2021).
[10] T. Karin, X. Linpeng, M.M. Glazov, M.V. Durnev, E.L. Ivchenko, S. Harvey, A.K. Rai, A. Ludwig, A.D. Wieck, Kai-Mei C. Fu. Phys. Rev. B **94**, 041201(R) (2016).
[11] P. Andreakou, A.V. Mikhailov, S. Cronenberger, D. Scalbert, A. Nalitov, A.V. Kavokin, M. Nawrocki, L.V. Butov, K.L. Campman, A.C. Gossard, M. Vladimirova. Phys. Rev. B **93**, 115410 (2016).
[12] M.V. Durnev, M.M. Glazov, X. Linpeng, M.L.K. Viitaniemi, B. Matthews, S.R. Spurgeon, P.V. Sushko, A.D. Wieck, A. Ludwig, Kai-Mei C. Fu. Phys. Rev. B **101**, 125420 (2020).
[13] E.L. Ivchenko. Optical Spectroscopy of Semiconductor Nanostructures. Alpha Science, Harrow (2005).
[14] A.V. Kavokin, J.J. Baumberg, G. Malpuech, F.P. Laussy, Microcavities. Oxford University, N.Y. (2007).
[15] C.F. Klingshirn. Semiconductor Optics. 4th ed. Springer, Berlin (2012).
[16] N. Tomassini, A. DeAndrea, R. Del Sole, H. Tuffigo-Ulmer, R.T. Cox. Phys. Rev. B **51**, 5005 (1995).
[17] E.S. Khramtsov, P.A. Belov, P.S. Grigoryev, I.V. Ignatiev, S.Yu. Verbin, Yu.P. Efimov, S.A. Eliseev, V.A. Lovtcius, V.V. Petrov, S.L. Yakovlev. J. Appl. Phys. **119**, 184301 (2016).
[18] A. Tredicucci, Y. Chen, F. Bassani, J. Massies, C. Deparis, G. Neu. Phys. Rev. B **47**, 10352 (1993).
[19] H.C. Schneider, F. Jahnke, S.W. Koch, J. Tignon, T. Hasche, D.S. Chemla. Phys. Rev. B **63**, 045202 (2001).
[20] G. Goger, M. Betz, A. Leitenstorfer, M. Bichler, W. Wegscheider, G. Abstreiter. Phys. Rev. Lett. **84**, 5812 (2000).
[21] M. Betz, G. Goger, A. Leitenstorfer, M. Bichler, G. Abstreiter, W. Wegscheider. Phys. Rev. B **65**, 085314 (2002).
[22] E.V. Ubyivovk, Yu.K. Dolgikh, Yu.P. Efimov, S.A. Eliseev, I.Ya. Gerlovin, I.V. Ignatiev, V.V. Petrov, V.V. Ovsyankin. J. Lumin. **102–103**, 751 (2003).
[23] E.V. Ubyivovk, D.K. Loginov, I.Ya. Gerlovin, Yu.K. Dolgikh, Yu.P. Efimov, S.A. Eliseev, V.V. Petrov, O.F. Vyvenko, A.A. Sitnikova, D.A. Kirilenko. FTT **51**, 1929 (2009). (in Russian).
[24] D. Schiumarini, N. Tomassini, L. Pilozzi, A. D'Andrea. Phys. Rev. B **82**, 075303 (2010).
[25] E.S. Khramtsov, P.S. Grigoryev, D.K. Loginov, I.V. Ignatiev, Yu.P. Efimov, S.A. Eliseev, P.Yu. Shapochkin, E.L. Ivchenko, M. Bayer. Phys. Rev. B **99**, 035431 (2019).
[26] S. Schumacher, G. Czycholl, F. Jahnke, I. Kudyk, H.I. Ruckmann, J. Gutowski, A. Gust, G. Alexe, D. Hommel. Phys. Rev. B **70**, 235340 (2004).
[27] M. Nakayama, D. Kim, H. Ishihara. Phys. Rev. B **74**, 073306 (2006).
[28] A.V. Trifonov, S.N. Korotan, A.S. Kurdyubov, I.Ya. Gerlovin, I.V. Ignatiev, Yu.P. Efimov, S.A. Eliseev, V.V. Petrov, Yu.K. Dolgikh, V.V. Ovsyankin, A.V. Kavokin. Phys. Rev. B **91**, 115307 (2015).
[29] D.K. Loginov, A.V. Trifonov, I.V. Ignatiev. Phys. Rev. B **90**, 075306 (2014).
[30] D.K. Loginov, P.S. Grigoryev, Yu.P. Efimov, S.A. Eliseev, V.A. Lovtcius, V.V. Petrov, E.V. Ubyivovk, I.V. Ignatiev. Phys. Status Solidi B **253**, 1537 (2016).
[31] S. Zielinska-Raczynska, D. Ziemkiewicz, G. Czajkowski. Phys. Rev. B **97**, 165205 (2018).
[32] D.K. Loginov, P.A. Belov, V.G. Davydov, I.Ya. Gerlovin, I.V. Ignatiev, A.V. Kavokin, Y. Masumoto. Phys. Rev. Res. **2**, 033510 (2020).
[33] D.K. Loginov, A.V. Donets. FTT **63**, 457 (2021). (in Russian).
[34] S.Yu. Bodnar, P.S. Grigoryev, D.K. Loginov, V.G. Davydov, Yu.P. Efimov, S.A. Eliseev, V.A. Lovtcius, E.V. Ubyivovk, V.Yu. Mikhailovskii, I.V. Ignatiev. Phys. Rev. B **95**, 195311 (2017).
[35] D. Loginov, V.P. Kochereshko, A. Litvinov, L. Besombes, H. Mariette, J.J. Davies, L.C. Smith, D. Wolverson. Acta Phys. Pol. A **112**, 381 (2007).
[36] J.J. Davies, D. Wolverson, V.P. Kochereshko, A.V. Platonov, R.T. Cox, J. Cibert, H. Mariette, C. Bodin, C. Gourgon, E.V. Ubyivovk, Y.P. Efimov, S.A. Eliseev. Phys. Rev. Lett. **97**, 187403 (2006).
[37] P.S. Grigoryev, O.A. Yugov, S.A. Eliseev, Yu.P. Efimov, V.A. Lovtcius, V.V. Petrov, V.F. Sapega, I.V. Ignatiev. Phys. Rev. B **93**, 205425 (2016).
[38] Evan O. Kane. Phys. Rev. B **11**, 3850 (1975).
[39] V.N. Tchelomey. Vibratsii v tekhnike. Mashinostroenie, M. (1978). (in Russian).
[40] I. Vurgaftman, J.R. Meyer, L.R. Ram-Mohan. J. Appl. Phys. **89**, 5815 (2001).
[41] G.E. Stillman, D.M. Larsen, C.M. Wolfe, R.C. Brandt. Solid State Commun. **9**, 2245 (1971).
[42] G.E. Pikus, V.A. Marushchak, A.N. Titkov. FTP, **22**, 185 (1988). (in Russian).

Translated by E.Ilinskaya